

See discussions, stats, and author profiles for this publication at: <https://www.researchgate.net/publication/235795790>

Infrared Spectroscopy with Heated Attenuated Total Internal Reflectance Enabling Precise Measurement of Thermally Induced Transitions in Complex Biological Polymers

ARTICLE in ANALYTICAL CHEMISTRY · MARCH 2013

Impact Factor: 5.64 · DOI: 10.1021/ac303552s · Source: PubMed

CITATIONS

11

READS

274

5 AUTHORS, INCLUDING:



Frederick J Warren

Institute of Food Research

32 PUBLICATIONS 200 CITATIONS

SEE PROFILE



Paul G Royall

King's College London

81 PUBLICATIONS 1,042 CITATIONS

SEE PROFILE



Peter J Butterworth

King's College London

158 PUBLICATIONS 1,290 CITATIONS

SEE PROFILE



Peter R Ellis

King's College London

98 PUBLICATIONS 2,314 CITATIONS

SEE PROFILE

Infrared Spectroscopy with Heated Attenuated Total Internal Reflectance Enabling Precise Measurement of Thermally Induced Transitions in Complex Biological Polymers

Frederick J. Warren,[†] Benjamin B. Perston,[‡] Paul G. Royall,[§] Peter J. Butterworth,[†] and Peter R. Ellis^{*,†}

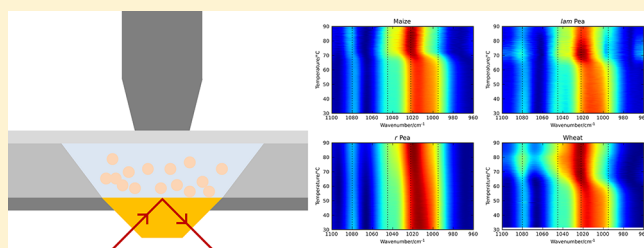
[†]King's College London, School of Medicine, Diabetes and Nutritional Sciences Division, Biopolymers Group, London, Franklin-Wilkins Building, 150 Stamford Street, London, SE1 9NH, United Kingdom

[‡]PerkinElmer, Chalfont Road, Seer Green, Buckinghamshire, HP9 2FX, United Kingdom

[§]King's College London, Institute of Pharmaceutical Science, Drug Delivery Group, Franklin-Wilkins Building, 150 Stamford Street, London, SE1 9NH, United Kingdom

S Supporting Information

ABSTRACT: We report an improved tool for acquiring temperature-resolved fourier transform infrared (FT-IR) spectra of complex polymer systems undergoing thermal transitions, illustrated by application to several phenomena related to starch gelatinization that have proved difficult to study by other means. Starch suspensions from several botanical origins were gelatinized using a temperature-controlled attenuated total reflectance (ATR) crystal, with IR spectra collected every 0.25 °C. By following the 995/1022 cm⁻¹ peak ratio, clear transitions occurring between 59 and 70 °C were observed, for which the midpoints could be determined accurately by sigmoidal fits. The magnitude of the change in peak ratio was found to be strongly correlated to the enthalpy of gelatinization as measured by differential scanning calorimetry (DSC, $R^2 = 0.988$). An important advantage of the technique, compared to DSC, is that the signal-to-noise ratio is not reduced when measuring very broad transitions. This has the potential to allow more precise determination of the gelatinization parameters of high-amylose starches, for which gelatinization may take place over several tens of °C.



Fourier transform infrared spectroscopy with attenuated total reflectance (FT-IR-ATR) is widely used in physical and analytical chemistry for studying forms of materials that are difficult to study by conventional means, such as films, interfaces, and suspensions.^{1–3} The recent commercial availability of temperature-controlled ATR spectrometer accessories opens a new class of applications to study by this method. The ability to hold the sample at a fixed temperature or to scan accurately across a wide range of temperatures allows high-quality spectral data to be collected in situ from complex materials undergoing structural changes during heating, offering new insights into important processes such as glass transitions and sol–gel transitions.⁴

In the present paper, starch gelatinization is used as an example of a complex polymer system, in the form of a suspension, undergoing a temperature-induced transition from an ordered structure to an amorphous gel-like form. Monitoring starch gelatinization by measuring changes in heatflow^{5–7} or mechanical strength⁸ allows accurate determination of transition temperatures and enthalpies, but little molecular information is provided, and sample presentation may significantly influence the results that are obtained with these techniques. Although spectroscopy has given insights into how the conformation and packing of starch molecules change

during gelatinization,^{2,9,10} a hyphenated, in situ technique is required that will allow the simultaneous characterization of both the chemical and the physical changes accompanying starch gelatinization and similar temperature-induced structural changes in related systems. Heated FT-IR-ATR has been recognized as a method that can provide detailed information on phase transitions since the early 1980s with the development of Fourier Transform instruments that could obtain spectra quickly enough to allow spectral changes to be monitored during sample heating.¹¹ Heated FT-IR-ATR has subsequently been used to monitor phase transitions, such as glass transitions, crystallization, and melting in a range of materials.^{4,12–14}

Starch is the primary storage polymer in all higher plants and forms an important part of the human diet, as well as playing a key role in a number of industrial processes. Thus, the chemistry of its transitions is important to understand for optimization and development purposes. Starch is the main source of energy in the human diet in the form of exogenous glucose. The significance of starch gelatinization has been

Received: December 21, 2012

Accepted: March 5, 2013

Published: March 5, 2013



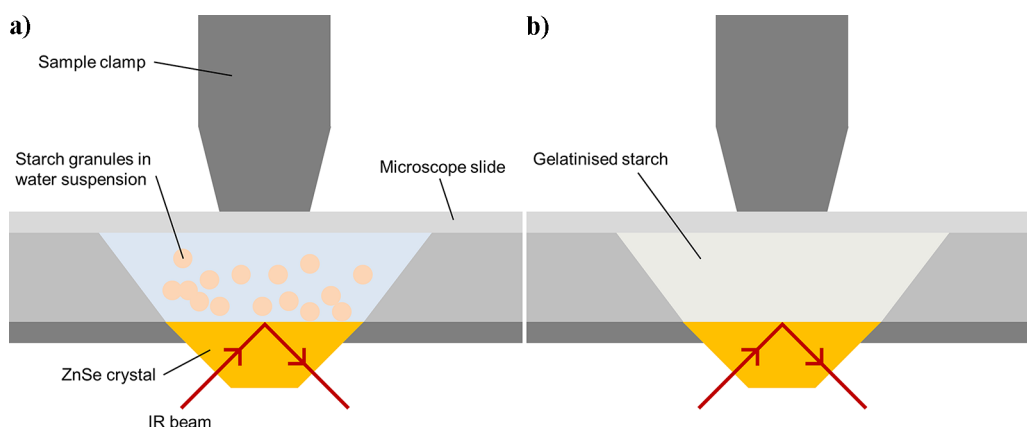


Figure 1. (a) Schematic showing the heated ATR experimental setup. The ATR crystal is shown in yellow, with the direction of the infrared beam shown in red. Individual starch granules (not to scale) are nominally suspended in water, but there is a degree of settling onto the crystal. The well is covered with a microscope slide held in place by the pressure clamp indicated in gray. (b) After gelatinization, the starch is no longer present as discrete granules and is distributed throughout the sample cell in a gel-like form.

implicated both in early stages of human evolution¹⁵ and in the detrimental health effects of a modern western high glycemic index diet, including increased risks of developing type II diabetes, cardiovascular disease, and obesity.^{16,17} Starch is also a key feedstock for bioethanol production¹⁸ and brewing,¹⁹ where the starch must be gelatinized and saccharified in order to be utilized. When starch is heated in excess water, it undergoes a dramatic structural change termed gelatinization, at a temperature that is characteristic of the botanical origin of the starch and which lies typically between 50 and 80 °C. Gelatinization is a fundamentally different process from the melting of whole starch granules. The latter process occurs in the absence of any plasticizing agent such as water at much higher temperatures of 130–170 °C. For crystallites that are anhydrous, melting temperatures can be even higher.^{20–23} Starch gelatinization is believed to be initiated by absorption of water by the amorphous regions of the starch granule, leading to swelling. This swelling destabilizes the crystalline regions of the starch granule and results in a complete loss of molecular order, as evidenced by the loss of X-ray and neutron scattering patterns.^{20,22,24} Gelatinization and crystallite melting are endothermic transitions and may be measured by differential scanning calorimetry (DSC).^{7,20,25,26}

Early work identified the region 1300–800 cm^{-1} of the mid-infrared (MIR) spectra of starch, where there are a number of absorbance bands related to C–C and C–O stretching and C–O–H bending modes.²⁷ Although these bands are yet to be fully assigned and the analysis is complicated by spectral overlap, it has been known for some years that several bands in this region are sensitive to the crystallinity of the starch. Broadly, bands have been assigned to either the amorphous or the crystalline form, and band ratios have been used to provide a measure of crystallinity.² The principal band associated with the amorphous form is at 1022 cm^{-1} ,²⁷ while shoulders at 1045 and ~995 cm^{-1} have been assigned to crystalline starch.^{2,28} More recently, Capron and co-workers²⁸ reported that the absorbance ratio 1000:1022 cm^{-1} from FT-IR-ATR measurements correlated well with the crystallinity index determined by X-ray powder diffraction for lintnerized, granular, and extruded starches at various water contents.

Conventional FT-IR-ATR approaches for the study of the structural differences between native (uncooked) and gelatinized starches is limited to heating the starch samples to

specific temperatures around their gelatinization point, cooling to room temperature, and then scanning.^{2,29,30} While this approach has demonstrated the usefulness of infrared measurements, it is time-consuming, lacks thermal resolution, and risks errors introduced due to starch retrogradation (recrystallization) during cooling. Transmission FT-IR has also been used to monitor temperature–pressure induced gelatinization.^{31,32} One research group has published results obtained with a temperature-controlled ATR device,³³ but their equipment had severely limited spectral resolution (between 100 and 19 cm^{-1}), meaning that relatively sparse information was obtained about the order–disorder transitions that occur during gelatinization. As a result, while the authors were able to estimate the temperature at which the transition occurred, they were unable to quantify structural changes in the starch during heating.

The spectrum of a starch suspension in water is dominated by the presence of major OH absorbance bands arising from OH bond stretching (3700–3000 cm^{-1}) and bending (1640 cm^{-1})^{34–37} modes of water. The bending mode at 1640 cm^{-1} shows only limited temperature sensitivity, while the stretching band at 3700–3000 cm^{-1} undergoes dramatic changes during heating due to its sensitivity to changes in hydrogen bonded structures.^{36,37} The structure of the OH stretching band is highly sensitive to changes in hydrogen bonding structure within an aqueous sample, and it has previously been suggested that changes in its structure may be used to probe hydrogen bonding interactions between water and polymers in aqueous polymer systems.^{4,38–40}

A number of different models have been suggested to fit the complex OH stretching band, which is composed of several peaks, describing a range of different water structures with varying degrees of order.³⁷ A common approach decomposes the band into three Gaussian peaks associated with different degrees of order in the hydrogen bonding structure.³⁷ At low temperatures, the predominant state of the water molecules is highly coordinated, with an H-bond coordination close to four (as is seen in ice), termed “network water”. As the temperature increases, the balance shifts toward a more loosely connected state in which the water molecules are isolated from their surroundings, called “multimer water”. Between these two states lies a third component, “intermediate water”, which forms an average number of H bonds. The Gaussian peaks are

positioned at approximately 3590 cm^{-1} (multimer), 3460 cm^{-1} (intermediate), and 3295 cm^{-1} (network).³⁷

In this paper, we explore the use of a temperature-controlled ATR device to investigate the molecular changes that occur during starch gelatinization *in situ*, both in excess water and under limited water conditions. Additionally, we explore the changes that occur to water structure during heating and the influence this may have on starch gelatinization. This work aims to develop a hyphenated heated ATR method to provide spectroscopic information on starch structure during gelatinization, allowing more detailed information than has previously been possible to be obtained on this structural transition. It is envisaged that this method could also be applied to other polymer systems that undergo thermal transitions.

MATERIALS AND METHODS

All water used was ultrapure deionized from a Millipore system, with an electrical resistivity of $18.2\text{ M}\Omega\cdot\text{cm}$. For details of the sources of starches (wheat, potato, maize, wild type (WT) pea, and *lam* and *r* mutant pea) used in this study and methods for characterization of starches by DSC and thermogravimetric analysis (TGA), see the Supporting Information.

Temperature-Controlled FT-IR-ATR. All spectra were collected using a PerkinElmer Spectrum Two FT-IR spectrophotometer, fitted with a resistively heated Pike MIRacle single-reflection ATR device, with a ZnSe crystal. Data were collected using a PC to run PerkinElmer TimeBase software. The same PC was also used to run Pike TempPRO software, which was used to control the heated ATR crystal and collect temperature data.

Starch samples were prepared by suspending 100 mg of starch in up to 1 mL of water. One hundred microliters of the starch suspension was pipetted into a PTFE sample well attached to the top of the ATR device so that the suspension was presented directly to the ATR crystal (Figure 1). The sample well was covered with a glass microscope slide, which was held in place with the ATR sample clamp to create a water tight seal, minimizing loss of water during the experiment. The temperature of the sample closely matched the reported temperature of the crystal, as verified by running an experiment with a thermocouple immersed in the sample.

Spectra were collected from 4000 to 650 cm^{-1} at a resolution of 4 cm^{-1} . A background spectrum consisting of 8 co-added scans ($\sim 40\text{ s}$) was obtained after cleaning the crystal with water and isopropanol. Samples were heated from 30 to $90\text{ }^{\circ}\text{C}$ at a rate of $3\text{ }^{\circ}\text{C}/\text{min}$. During heating, spectra were collected at a rate of approximately one every 5 s , equating to approximately 4 spectra per degree of heating. The thermocouple readout and the recorded sample temperature matched to within $0.5\text{ }^{\circ}\text{C}$ throughout heating.

Data were analyzed using TimeBase, Spectrum 10, and GNU Octave.⁴¹ Prior to display as heat maps, spectra were processed by baseline correction and normalization. Baseline correction was effected iteratively by fitting a straight line to each spectrum in the range of 1130 – 960 cm^{-1} , deleting the points above the line, and then repeating the fit, with the final baseline then subtracted from the spectrum. Fifty iterations were found to give adequate results. The baseline-corrected spectra were vector normalized by dividing each spectrum by the standard deviation of its absorbance values (without mean subtraction). Band ratios were likewise calculated from the baseline-corrected spectra.

Sigmoidal curves were fit to the band ratio profiles using a Nelder-Mead simplex optimization function implemented in GNU Octave to minimize the sum-squared error of the fit. The same approach was used to fit Gaussian peaks to the OH stretching region of selected spectra. Peak positions, heights, and widths were allowed to vary in the fit to pure water at $30\text{ }^{\circ}\text{C}$, and then, the peak positions were fixed for the fits to the other samples.

RESULTS

Changes in the FT-IR-ATR Spectrum of Starch as a Result of Heating in Excess Water. Examples of the spectra obtained during heating of maize starch are shown in Figure S-1, Supporting Information. A number of spectral features changed over the course of the experiment. The spectra are dominated by absorption bands due to stretching and bending modes of water, at 3700 – 3000 and 1640 cm^{-1} , respectively (Figure S-1a, Supporting Information). These bands are known to change with temperature, reflecting changes in the hydrogen bonding structure of water, and this phenomenon has been studied in detail before.^{36,37,42} The questions of whether this behavior is affected by the presence of starch and whether the O–H modes of starch itself can readily be observed will be addressed later in this paper. The most important absorption bands of starch are due to C–C and C–O stretching modes and C–O–H bending modes and are observed in the region of 1300 – 800 cm^{-1} (Figure S-1b, Supporting Information).

The region of interest is shown in detail in Figure 2. The spectrum of native starch shows peaks at 995 and 1022 cm^{-1} ,

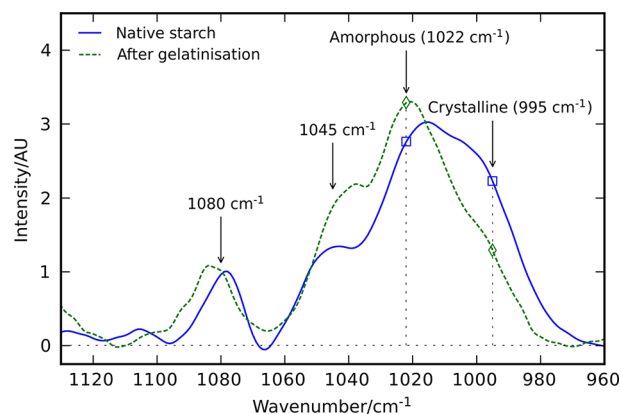


Figure 2. Details of baseline-corrected and vector normalized spectra of native and gelatinized maize starch. The frequencies used for the ratio calculation are indicated by open symbols.

with a shoulder at 1045 cm^{-1} . Heating results in dramatic changes to the spectra. A general reduction in the intensity of the whole starch spectrum may clearly be observed in Figure S-1, Supporting Information, and can be explained by the properties of the ATR experiment and the change in the form of the sample. One of the principal characteristics of ATR measurements is the very short penetration of the radiation into the sample. The intensity decreases exponentially with depth and falls to $1/e$ of its value at the surface at around $2\text{ }\mu\text{m}$ for the system under study here (see Equation S-1 in the Supporting Information). This distance is very much less than the depth of the sample. The extent to which the sampled region is representative of the entire sample must be evaluated. The starch samples used in this study ranged from 17 to $60\text{ }\mu\text{m}$ in

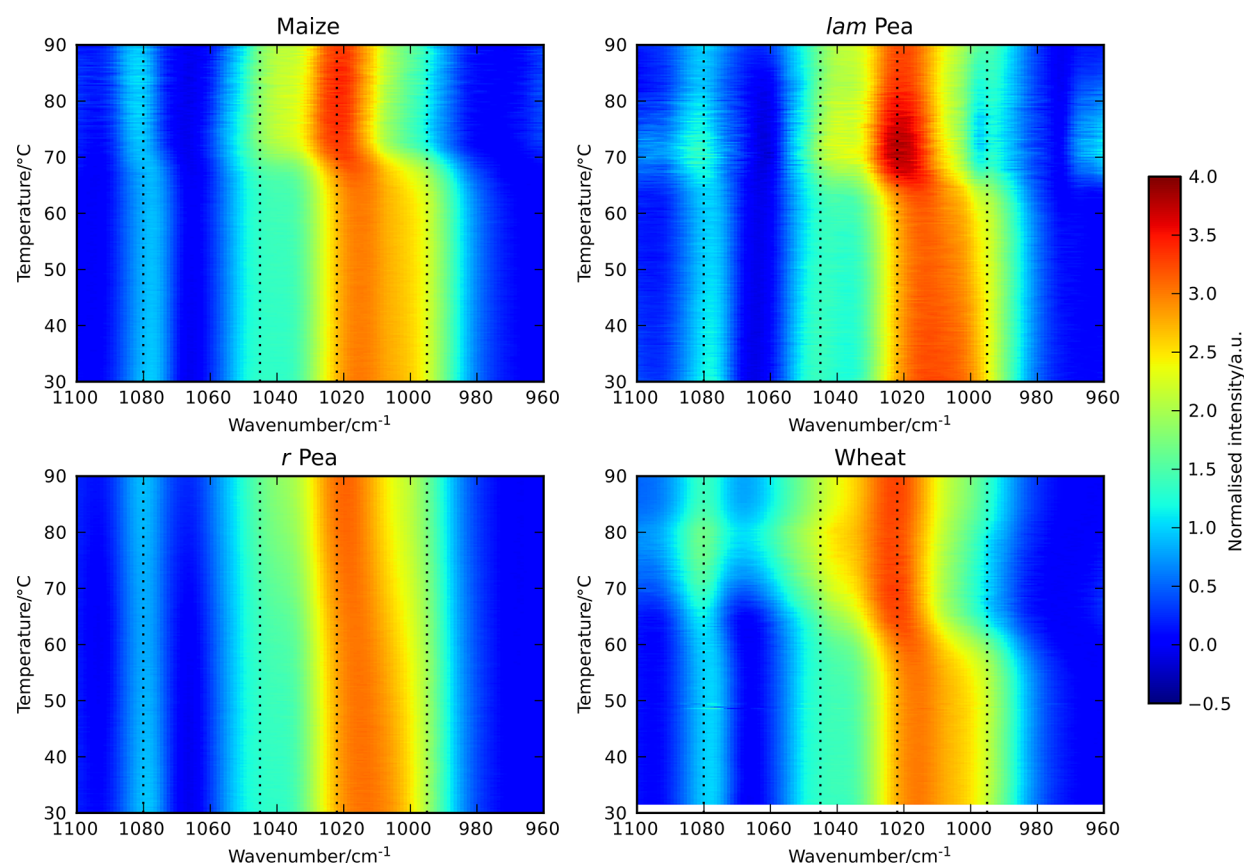


Figure 3. Heat maps showing the changes in the spectra of maize, wheat, *lam* mutant pea, and *r* mutant pea starches that occur as a function of temperature. The dotted lines indicate the peaks marked in Figure 2.

mean diameter,⁵ so the beam penetrated the surface of the granule to a depth of 5–10% of the granule diameter.

Prior to gelatinization, the starch granules settle to the bottom of the cell, increasing the amount of starch in the region of the liquid cell sampled by the ATR crystal (Figure 1a). During gelatinization, the starch granules swell and leach α -glucan polymer, resulting in a relatively uniform gel in which the starch is distributed throughout the whole liquid cell (Figure 1b). As a result, there is less starch in the area sampled by the ATR crystal, and an overall reduction in the intensity of starch bands. This explanation is supported by the results for maize starch heated with a low (41%, w/w) water content. Under these conditions, the starch fails to gelatinize fully and maintains its granular structure, and no reduction in signal intensity is observed (data not shown).

Vector normalization removes the effect of this intensity reduction, and a plot of the normalized spectra (Figure 2) shows clearly the changes in the relative heights of the starch peaks. Gelatinization results in a significant decrease at 995 cm^{-1} and increase at 1022 cm^{-1} . The peak at around 1080 cm^{-1} , also previously reported to depend on the crystallinity,^{31,32} appears to grow broader and weaker and shift to higher wavenumber.

The evolution of the spectra with time is depicted in the heat maps of Figure 3, which reveal that the transition from native to gelatinized starch spectra is clearly defined and occurs over a narrow temperature range, as the starch structure rapidly changes from a more ordered to a more amorphous form. It is clear that for wheat, potato, maize, and WT and *lam* pea starches there is a defined shift in the peak absorbance from

995 toward 1022 cm^{-1} when the starch undergoes gelatinization. This change also occurs in the *r* pea starch but is less pronounced and occurs over a wider temperature interval.

The 995/1022 cm^{-1} band ratios and sigmoid fits plotted in Figure 4 show, for all samples except *r* pea showing a sharp drop around the gelatinization temperature. A similar result was observed for the 1045/1022 cm^{-1} ratio (data not shown), as has been used previously in pressure–temperature studies of starch gelatinization by FT-IR,^{31,32} but the signal-to-noise ratio is poorer than for 995/1022 cm^{-1} . It was previously observed²⁸

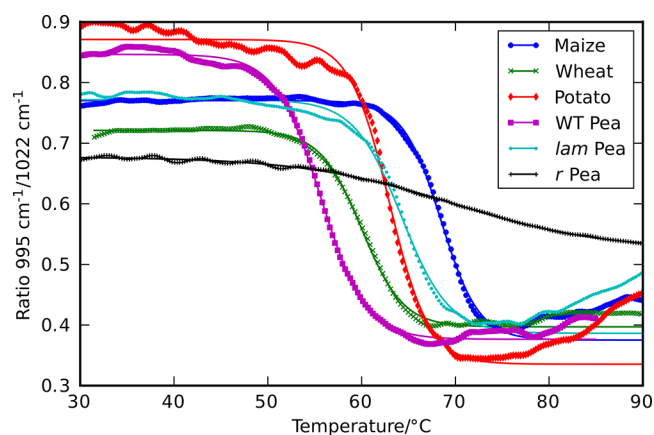


Figure 4. Ratio of absorbance intensities at 995 cm^{-1} /1022 cm^{-1} plotted as a function of temperature for maize, wheat, potato, wild type pea, *lam* mutant pea, and *r* mutant pea starches. Sigmoidal best-fit curves are shown as solid lines.

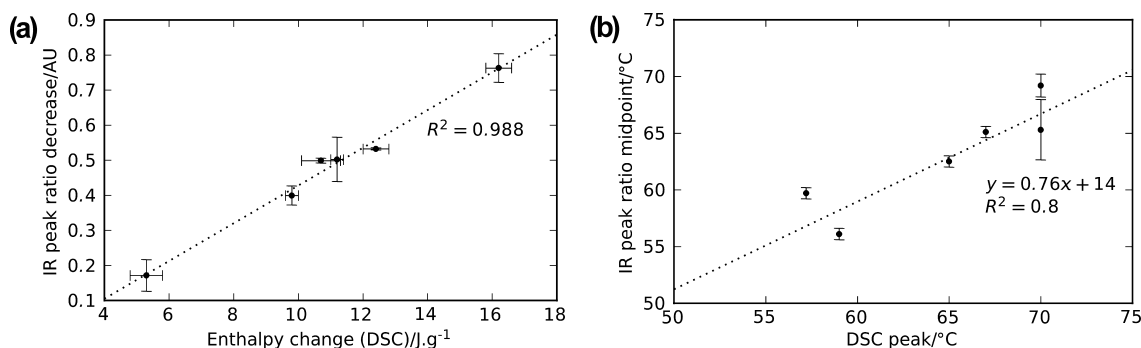


Figure 5. (a) Relationship between the decrease in the IR ratio $995\text{ cm}^{-1}/1022\text{ cm}^{-1}$ during gelatinization of all starches and the enthalpy change for the same transition observed by DSC. (b) Relationship between the midpoint of the transition observed in the infrared spectra and the peak temperature of starch gelatinization as measured by DSC. Error bars indicate \pm standard error of the mean (SEM) from triplicate determinations.

that the ratio $995/1022\text{ cm}^{-1}$ is a more sensitive measure of structure than $1045/1022\text{ cm}^{-1}$, and the present data seem to confirm this.

Comparison with DSC Measurements. Temperatures for the midpoint, onset, and conclusion of gelatinization measured by infrared, in addition to the band ratio decrease, were obtained by sigmoidal fitting to a plot of $995/1022\text{ cm}^{-1}$ band ratio against temperature (Figure 4). These data are shown for a diverse range of starches in Table S1, Supporting Information, where good agreement with onset and conclusion temperatures determined by DSC is demonstrated across a wide range of gelatinization temperatures. It is interesting to note that, while the native-starch band ratio values vary over a relatively wide range, following gelatinization the starch band ratios (with the exception of *r* pea) are much more homogeneous, having a value of approximately 0.4 independent of the value before gelatinization (Figure 4). This value may be typical of completely amorphous, disordered starch, regardless of its botanical origin. A similar value of 0.4 was obtained by Sevenou and co-workers² for gelatinized and cooled starch. However, it should also be noted that the absolute value for the band ratio is dependent on the method of baseline correction used (the results will be internally consistent as long as a consistent method of baseline correction is used throughout all analyses).

If the $995:1022\text{ cm}^{-1}$ band ratio is an infrared indicator of starch ordered structure, then it could be expected that the magnitude of the decrease in band ratio offers a quantitative measure of the loss of ordered structure that occurs during gelatinization. An established method to quantify this property is the enthalpy change associated with the gelatinization DSC peak.^{6,7,20,43} Figure 5a shows very good correlation between the band ratio drop and DSC enthalpy change ($R^2 = 0.988$), indicating that the infrared data provide an accurate measure of the loss of ordered structure during gelatinization, although the value is not directly interpretable in energy terms without calibration. A somewhat weaker but still significant correlation was obtained between the transition midpoint temperatures measured by IR and DSC (Figure 5b: $R^2 = 0.8$, slope ≈ 1). These results constitute strong evidence that the loss of order observed spectroscopically is the same as the endothermic crystal melting transition that is seen by DSC.

A Tool for Investigation of Challenging Gelatinization Phenomena such as Starches from Mutant Plant Sources. Genetic manipulation has resulted in a wide range of starches with different compositions (particularly differences in amylose–amylopectin ratios) and, correspondingly, diverse functional properties. An extreme example of this is the *r*

mutant pea starch, which has approximately 70% amylose, compared to 31.9% amylose in wild type pea.⁸ The IR data reveal that the structural changes that occur in *r* pea starch during heating, while similar to those seen for other starches, happen in a somewhat different way. As observed by DSC, the *r* pea transition is a long, shallow one, occurring over a temperature interval approximately 3 times broader than that seen for other starches.⁴⁴ DSC results indicate only a small loss of order occurring during this transition, but IR spectroscopy provides a more detailed picture. Figure 4 shows that a sigmoidal curve has an excellent fit to the *r* pea data, allowing the onset, peak, and conclusion temperatures for the transition to be determined far more accurately than is possible using DSC alone. The *r* pea band ratio prior to gelatinization (Figure 4) suggests that, in the native form, *r* pea has a significantly less ordered structure than the other starch samples used in the present study, thus supporting previous findings.^{45,46} Interestingly, post-gelatinization, the *r* pea data did not converge with the other starches used and clearly retained a significantly ordered structure, an observation supported by optical microscopy studies reported by previous workers.⁴⁶ The fundamental advantage of IR spectroscopy in this case is that calorimetry depends on measuring a heat flow, which is necessarily weak if the transition is slow, while IR spectroscopy offers a direct probe of the structure (an intrinsic property) and is unaffected by the rate at which the transition occurs.

Starch Gelatinization in Limiting-Water Conditions. As described in the introduction, starch gelatinization is dependent on water, and complete gelatinization requires excess water to be present. In the anhydrous state, starch crystallites undergo melting at a much higher temperature, while intermediate water conditions result in partial gelatinization.^{21,23} To investigate the importance of the amount of water present, maize starch was heated at three different moisture contents. When equilibrated at laboratory humidity ($\sim 60\%$ R.H.) and temperature ($\sim 21^\circ\text{C}$), the maize starch was found thermogravimetrically to have a water content of 11.6% (w/w). Water was added, and the samples were left overnight to equilibrate, to give water contents of 41%, 56%, and 90% (w/w) water, representing limiting, intermediate, and excess water conditions, respectively. As shown above, in excess water, maize starch undergoes a single, clear transition at $\sim 70^\circ\text{C}$ with an associated enthalpy change of 10.7 J/g (Table S-1, Supporting Information). At intermediate water content (56%, w/w), the change in $995:1022\text{ cm}^{-1}$ band ratio was very similar to that seen with excess water. This observation is consistent with the DSC enthalpy change of 9.6 J/g (Table S-1, Supporting Information)

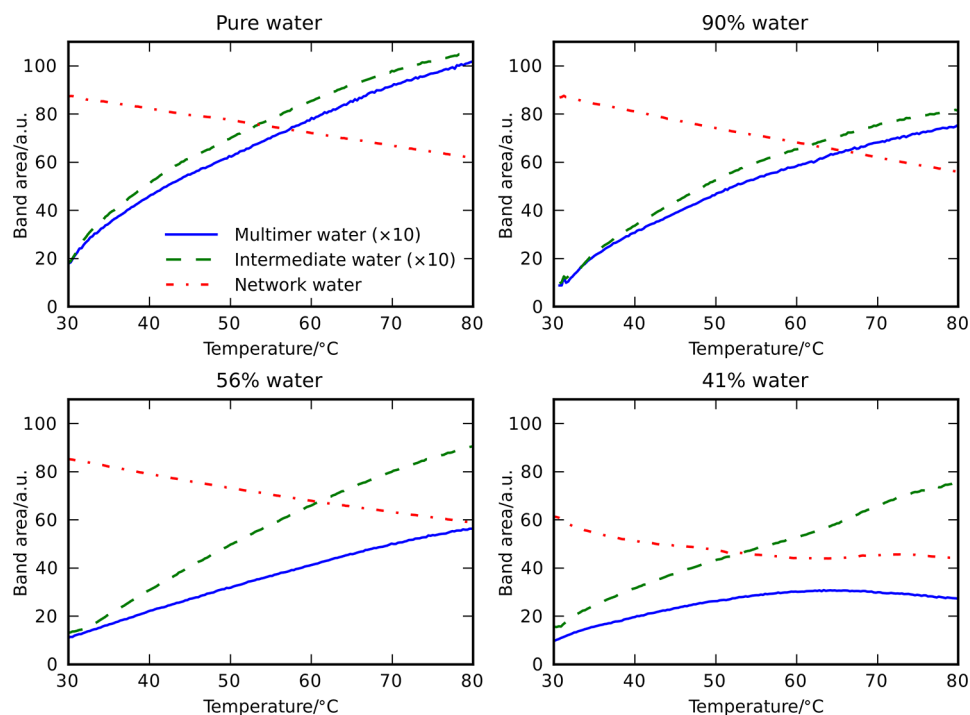


Figure 6. Decomposition of the OH stretching band for pure water and maize starch suspensions. Evolution of the fitted parameters during heating of starch suspensions with 41%, 56%, and 90% (w/w) water content. Note that the curves for intermediate and multimer water are shown with a scaling factor of 10 for clarity.

and indicates that, at this intermediate water content, there is still adequate water present for almost complete gelatinization of maize starch.

In contrast, in the restricted water regime, there was a relatively small enthalpy change of 1.3 J/g and a correspondingly small decrease in the IR band ratio, indicating that the majority of the starch remains in an ordered state during heating under such low water conditions (Figure S-2, Supporting Information).

A starch suspension is a two-phase system with insoluble starch granules mixed with water. It has previously been suggested that some of the changes observed in the OH stretching mode region of the spectra of starch suspensions may be due to the gelatinization of starch.³³ If this is the case, some dependence on the proportions of water and starch would be expected. For the spectral data sets from each of the maize samples, the OH stretching peak was decomposed into three Gaussian peaks, as described above.³⁷ Examples of the curve fitting are given for pure water and a starch suspension with 41% water at 30 and 80 °C in Figure S-3, Supporting Information. The areas of the three fitted peaks are plotted in Figure 6. The relative areas indicate the amounts of network, intermediate, and multimer water that are present, although it should be noted that this model is not considered closely representative of the structure of water but rather as a useful qualitative indication of the degree of order in the structure.

As pure water is heated, there is a clear increase in the relative amounts of intermediate and multimer water, as the increase in temperature reduces the strength of the hydrogen bonding network in the water, a phenomenon that is well described in the literature.^{36,37,42} When starch is included, the temperature profile of the OH stretching band is altered. The most obvious difference is that the intensity of the OH band at all temperatures is much lower for the samples with lower water

content. This observation may be explained by considering that starch consists of linked glucose units, each sugar ring having 3 OH groups and molar mass of 179 g/mol. The density of starch is around 1.5 g/mL,⁴⁷ so the volume density of OH groups is ~ 25 mol/L for pure starch. Water has 2 OH groups per molecule, a molar mass of 18, and a density of 1 g/mL. The volume density of OH groups in water, therefore, is ~ 111 mol/L. Increasing the starch concentration will have the effect of reducing the volume concentration of OH groups, explaining the reduction in the OH signal observed at the crystal surface. An interesting corollary to this is that the volume density of OH groups in starch relative to water is so low that, taking into account the limited penetration of the infrared beam into the starch, starch OH groups are unlikely to make a significant contribution to the OH stretching band. Hence, any changes in the OH stretching band structure observed during heating of the starch suspension are likely to result from changes in the hydrogen bonding structure of the water itself as a result of starch–water interactions. This has previously been suggested to be the case for the heating of other polymer–water systems.^{4,38–40}

Figure 6 shows how the relative intensities of the 3 Gaussian peaks change during heating. For starch with excess and 56% (w/w) water, there is little difference in the relative peak areas (and therefore peak structure) compared with pure water across a broad range of temperatures. This is similar to the observations made by Maeda⁴⁰ that at low polymer concentrations there is little effect on the OH stretching band structure, as the spectrum is dominated by absorption by water that is not interacting with polymer. When water is at a lower concentration of 41% (w/w), however, differences emerge. At temperatures below the gelatinization temperature, the relative band intensities are similar to that observed for pure water (the OH band is dominated by absorption by free water,

i.e., that not interacting with starch). There is a dramatic change, however, at the gelatinization temperature (around 70 °C). Relative to conditions of high water concentration, there is an increase in the fractions of network and intermediate water and a corresponding decrease of multimer water. This indicates that, during and after gelatinization, there is an increase in the degree of hydrogen bonding between starch and water, involving a significant proportion of the total amount of water. A potentially useful consequence of this phenomenon is that, at high starch concentrations, it is possible to use the structure of the OH stretching band to measure the interactions between water and starch polymers as starch undergoes gelatinization.

■ DISCUSSION

FT-IR-ATR is an increasingly widely used technique for studying the molecular structure of starch and other biopolymers. The advantages of this instrument, namely, that it is flexible, simple, and relatively inexpensive, are well-known, and the data presented in this paper show that it is eminently suited to the study of starch gelatinization phenomena. While FT-IR-ATR has found widespread use for the study of native starch structure,^{2,28} and for heated and cooled starches,^{2,27,29,30,48} the extension described here to in situ measurements is significant because it avoids the risk of further structural changes (retrogradation) occurring during cooling.

The results presented here show that FT-IR-ATR is able to determine onset, midpoint, and conclusion temperatures for gelatinization transitions, providing temperature data approximately equivalent to that available from DSC measurements. However, the gelatinization range (conclusion minus onset) obtained by heated ATR was found to be somewhat narrower than that obtained by DSC. This equivalence has been demonstrated for a diverse collection of starch samples and in different gelatinization conditions. Furthermore, IR may actually provide superior results in the case of protracted thermal events such as the gelatinization of *r* pea starch, which can be challenging to characterize calorimetrically.^{44–46} The IR data shown here indicate that, unlike in other starches, gelatinization in *r* pea starch is not a cooperative process and instead proceeds in a gradual manner above 60 °C. This is consistent with enzyme kinetic data previously presented by our group for the *r* pea starch.⁴⁶

The absorbance ratio 995:1022 cm⁻¹ decreases during gelatinization, reflecting the transition from an ordered to a disordered state. Onset, midpoint, and conclusion temperatures for gelatinization can be determined by fitting a sigmoidal curve to a plot of this ratio against temperature. Materials that undergo slow gelatinization, such as the high amylose mutant *r* pea starch, give broad, weak DSC peaks with correspondingly greater uncertainty as to the peak location. Because IR spectroscopy is a structural probe, the signal strength is independent of the energy flow and weak thermal transitions are no more difficult to measure than strong ones. This is evidenced by the excellent sigmoidal fit to the *r* pea peak ratio data, although the present experiment did not permit sufficiently high temperatures to observe the gelatinization conclusion directly. IR spectroscopy is thus a valuable complementary technique to DSC when characterizing starches with unusual gelatinization behavior.

The magnitude of the decrease in the peak ratio was very well correlated ($R^2 = 0.988$) to the enthalpy change (area under the DSC peak), indicating that the relative enthalpies of

gelatinization for different starches can be established by this spectroscopic technique. Some confidence about the general applicability of the technique can be derived from the much greater spectral similarity among gelatinized starches than native starches; the peak ratios for all fully gelatinized starches were within the range of 0.34–0.40, while the native starches varied from 0.72 to 0.88, a range nearly three times wider.

The data presented in this paper demonstrate that the IR data can also provide a reliable indication of the relative enthalpies associated with gelatinization transitions. After gelatinization, the band ratio reaches a value that is relatively independent of the origin of the starch, indicating that the approach is not limited to a few specific types of starch.

It is interesting to look at a starch system that lacks significant free water. At a 41% (w/w) water content, only a very small DSC peak and small change in starch peak ratios by ATR are observed during gelatinization, supporting the well-known observation that at low moisture content starch fails to gelatinize fully due to the lack of available free water.^{21,22,24,43,49} At this water content, there is a distinct change in the shape of the OH stretching peak as the starch goes through gelatinization, possibly indicative of increased interactions between water and starch polymers post-gelatinization.

■ CONCLUSIONS

Temperature-controlled FT-IR-ATR spectroscopy was found to be a powerful tool for characterizing starch gelatinization transitions, providing temperature-resolved structural and (once calibrated) energetic information in good agreement with results obtained by DSC. The present technique has significant potential to add to our understanding of the complex changes that occur during starch gelatinization. The temperature at which molecular order is lost may be determined to a high degree of accuracy, in addition to the degree of loss of order, and with further improvements, a wealth of information could be obtained regarding this important transition. For example, repeating these experiments in D₂O would allow an estimation of the accessibility of starch hydroxyl groups to exchange before, during, and after gelatinization. Moreover, the use of heated ATR spectroscopy clearly has potential to be extended to a range of other systems that undergo thermal transitions, where the ability to accurately scan and hold temperature while obtaining spectroscopic data could prove an invaluable experimental tool. This could include, for example, the study of lipid bilayer structure by ATR spectroscopy,⁵⁰ where structural transitions are highly temperature sensitive, and the study of the temperature sensitivity of surface drug deposition on polylactic and poly(lactic glycolic acid) particles,⁵¹ as well as the temperature-induced transitions of other biopolymer systems.⁴

■ ASSOCIATED CONTENT

§ Supporting Information

Experimental details and additional figures and tables. This material is available free of charge via the Internet at <http://pubs.acs.org>.

■ AUTHOR INFORMATION

Corresponding Author

*Tel.: +44 (0) 207 848 4238. Fax: +44 (0) 207 848 4171. E-mail: peter.r.ellis@kcl.ac.uk. Address: Biopolymers Group, Diabetes and Nutritional Sciences Division, King's College

London, Franklin-Wilkins Building (Room 4.102), 150 Stamford Street, London, SE1 9NH, UK.

Notes

The authors declare no competing financial interest.

ACKNOWLEDGMENTS

The authors would like to thank Dr. Richard Spragg (PerkinElmer, UK) for helpful comments and discussions in the preparation of this manuscript.

REFERENCES

- (1) Hind, A. R.; Bhargava, S. K.; McKinnon, A. *Adv. Colloid Interface Sci.* **2001**, 93, 91–114.
- (2) Sevenou, O.; Hill, S. E.; Farhat, I. A.; Mitchell, J. R. *Int. J. Biol. Macromol.* **2002**, 31, 79–85.
- (3) Duc Hanh, B.; Neubert, R. H. H.; Wartewig, S. *Int. J. Pharm.* **2000**, 204, 145–150.
- (4) Murphy, S.; Leeke, G.; Jenkins, M. J. *Therm. Anal. Calorim.* **2012**, 107, 669–674.
- (5) Warren, F. J.; Royall, P. G.; Gaisford, S.; Butterworth, P. J.; Ellis, P. R. *Carbohydr. Polym.* **2011**, 86, 1038–1047.
- (6) Wang, T. L.; Bogracheva, T. Y.; Hedley, C. L. *J. Exp. Bot.* **1998**, 49, 481–502.
- (7) Bogracheva, T. Y.; Meares, C.; Hedley, C. L. *Carbohydr. Polym.* **2006**, 63, 323–330.
- (8) Warren, F. J.; Royall, P. G.; Butterworth, P. J.; Ellis, P. R. *Carbohydr. Polym.* **2012**, 90, 628–636.
- (9) Cooke, D.; Gidley, M. J. *Carbohydr. Res.* **1992**, 227, 103–112.
- (10) Lopez-Rubio, A.; Flanagan, B. M.; Gilbert, E. P.; Gidley, M. J. *Biopolymers* **2008**, 89, 761–768.
- (11) Roush, P. B. *SPIE Proc.* **1981**, 289, 124–127.
- (12) Ottenhof, M.-A.; MacNaughton, W.; Farhat, I. A. *Carbohydr. Res.* **2003**, 338, 2195–2202.
- (13) Lin, S.-Y.; Chen, K.-S.; Liang, R.-C. *Polymer* **1999**, 40, 2619–2624.
- (14) Xu, J.; Guo, B.-H.; Yang, R.; Wu, Q.; Chen, G.-Q.; Zhang, Z.-M. *Polymer* **2002**, 43, 6893–6899.
- (15) Perry, G. H.; Dominy, N. J.; Claw, K. G.; Lee, A. S.; Fiegler, H.; Redon, R.; Werner, J.; Villanea, F. A.; Mountain, J. L.; Misra, R.; Carter, N. P.; Lee, C.; Stone, A. C. *Nat. Genet.* **2007**, 39, 1256–1260.
- (16) Sluijs, I.; van der Schouw, Y. T.; van der A, D. L.; Spijkerman, A. M.; Hu, F. B.; Grobbee, D. E.; Beulens, J. W. *Am. J. Clin. Nutr.* **2010**, 92, 905–911.
- (17) Wolever, T. M.; Gibbs, A. L.; Mehling, C.; Chiasson, J.-L.; Connelly, P. W.; Josse, R. G.; Leiter, L. A.; Maheux, P.; Rabasa-Lhoret, R.; Rodger, N. W.; Ryan, E. A. *Am. J. Clin. Nutr.* **2008**, 87, 114–125.
- (18) Smith, A. M. *Plant J.* **2008**, 54, 546–558.
- (19) Bamforth, C. W. *J. Cereal Sci.* **2009**, 50, 353–357.
- (20) Bogracheva, T. Y.; Wang, Y. L.; Hedley, C. L. *Biopolymers* **2001**, 58, 247–259.
- (21) Roder, N.; Gerard, C.; Verel, A.; Bogracheva, T. Y.; Hedley, C. L.; Ellis, P. R.; Butterworth, P. J. *Food Chem.* **2009**, 113, 471–478.
- (22) Perry, P. A.; Donald, A. M. *Carbohydr. Polym.* **2002**, 49, 155–165.
- (23) Noel, T. R.; Ring, S. G. *Carbohydr. Res.* **1992**, 227, 203–213.
- (24) Jenkins, P. J.; Donald, A. M. *Carbohydr. Res.* **1998**, 308, 133–147.
- (25) Bogracheva, T. Y.; Wang, Y. L.; Wang, T. Y.; Hedley, C. L. *Biopolymers* **2002**, 64, 268–281.
- (26) Tananuwong, K.; Reid, D. S. *Carbohydr. Polym.* **2004**, 58, 345–358.
- (27) van Soest, J. J. G.; Tournois, H.; de Wit, D.; Vliegthart, J. F. G. *Carbohydr. Res.* **1995**, 279, 201–214.
- (28) Capron, I.; Robert, P.; Colonna, P.; Brogly, M.; Planchot, V. *Carbohydr. Polym.* **2007**, 68, 249–259.
- (29) Li, Y.; Shoemaker, C. F.; Ma, J.; Moon, K. J.; Zhong, F. *Food Chem.* **2008**, 106, 1105–1112.
- (30) Miao, M.; Zhang, T.; Mu, W.; Jiang, B. *Food Chem.* **2010**, 119, 41–48.
- (31) Rubens, P.; Heremans, K. *Biopolymers* **2000**, 54, 524–530.
- (32) Rubens, P.; Snaauwaert, J.; Heremans, K.; Stute, R. *Carbohydr. Polym.* **1999**, 39, 231–235.
- (33) Iizuka, K.; Aishima, T. *J. Food Sci.* **1999**, 64, 653–658.
- (34) Libnau, F. O.; Toft, J.; Christy, A. A.; Kvalheim, O. M. *J. Am. Chem. Soc.* **1994**, 116, 8311–8316.
- (35) Libnau, F. O.; Christy, A. A.; Kvalheim, O. M. *Appl. Spectrosc.* **1995**, 49, 1431–1437.
- (36) Freda, M.; Piluso, A.; Santucci, A.; Sassi, P. *Appl. Spectrosc.* **2005**, 59, 1155–1159.
- (37) Brubach, J. B.; Mermet, A.; Filabozzi, A.; Gerschel, A.; Roy, P. J. *Chem. Phys.* **2005**, 122, 184509–7.
- (38) Sammon, C.; Bajwa, G.; Timmins, P.; Melia, C. D. *Polymer* **2006**, 47, 577–584.
- (39) Maeda, H.; Ozaki, Y.; Tanaka, M.; Hayashi, N.; Kojima, T. *J. Near Infrared Spectrosc.* **1995**, 3, 191–202.
- (40) Maeda, Y. *Langmuir* **2001**, 17, 1737–1742.
- (41) See <http://www.gnu.org/software/octave/> for download (accessed 14 December 2012).
- (42) Walrafen, G. E. *J. Chem. Phys.* **1967**, 47, 114–126.
- (43) Donovan, J. W. *Biopolymers* **1979**, 18, 263–275.
- (44) Bogracheva, T. Y.; Davydova, N. I.; Genin, Y. V.; Hedley, C. L. *J. Exp. Bot.* **1995**, 46, 1905–1913.
- (45) Bogracheva, T. Y.; Cairns, P.; Noel, T. R.; Hulleman, S.; Wang, T. L.; Morris, V. J.; Ring, S. G.; Hedley, C. L. *Carbohydr. Polym.* **1999**, 39, 303–314.
- (46) Tahir, R.; Ellis, P. R.; Bogracheva, T. Y.; Meares-Taylor, C.; Butterworth, P. J. *Biomacromolecules* **2011**, 12, 123–133.
- (47) Dhital, S.; Shrestha, A. K.; Gidley, M. J. *Carbohydr. Polym.* **2010**, 82, 480–488.
- (48) Vliegthart, J.; Smits, A.; Ruhnau, F.; van Soest, J. J. G. *Starch-Stärke* **1998**, 50, 478–483.
- (49) Donovan, J. W.; Lorenz, K.; Kulp, K. *Cereal Chem.* **1983**, 60, 381–387.
- (50) Silvestro, L.; Axelsen, P. H. *Chem. Phys. Lipids* **1998**, 96, 69–80.
- (51) Royall, P. G.; Hill, V. L.; Craig, D. Q. M.; Price, D. M.; Reading, M. *Pharm. Res.* **2001**, 18, 294–298.